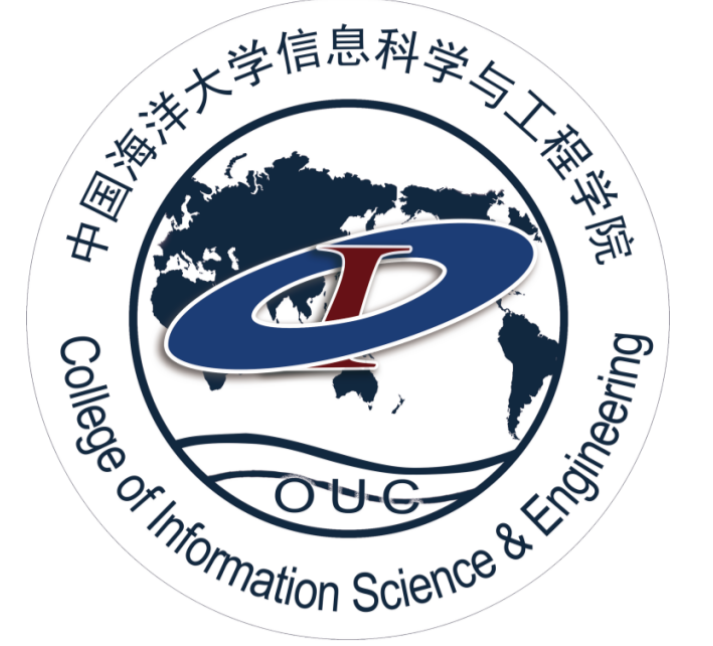




Generation of quasi-monoenergetic positron beams in chirped laser fields

Suo Tang

College of Physics and Optoelectronic Engineering, Ocean University of China, Qingdao, 266100, China



High energy photons can decay to electron-positron pairs via the nonlinear Breit-Wheeler process when colliding with an intense laser pulse. The energy spectrum of the produced particles is broadened because of the variation of their effective mass in the course of the laser pulse. Applying a suitable chirp to the laser pulse can narrow the energy distribution of the generated electrons and positrons. We present a scenario where a high-energy electron beam is collided with a chirped laser pulse to generate a beam of quasi-monoenergetic γ -photons, which then decay in a second chirped, UV pulse to produce a quasi-monoenergetic source of high-energy electrons and positrons.

Nonlinear Breit-Wheeler Pair Production

We consider the scenario in which a high-energy photon with momentum ℓ^μ colliding (almost) head-on with a laser pulse k^μ produces a pair of electron and positron. The interaction energy is characterised by $\eta_\ell = k \cdot \ell / m^2$.

The angular-resolved spectrum of the produced positron can be formulated as

$$\frac{d^3P}{dsd^2q_\perp} = \alpha \frac{|I|^2 + (SI^* + IS^* - 2F \cdot F^*)g(s, 1)}{(2\pi)^2 \eta_\ell^2 (1-s)s}, \quad (1)$$

where $g(u, v) = [u^2 + (v-u)^2]/[4u(v-u)]$, $s = k \cdot p / k \cdot \ell$, and $q_\perp = (q_x, q_y)$, $q_{x,y} = p_{x,y}/m - s\ell_{x,y}/m$. For small angle collisions $\ell_\perp \approx 0$, $q_\perp \approx \gamma_p \theta_p (\cos \psi, \sin \psi)$ where θ_p and ψ are the polar and azimuthal angles, and γ_p is the positron energy factor. The functions I , F and S are defined as

$$I = \int d\phi \left(1 - \frac{\ell \cdot \pi_p}{\ell \cdot p}\right) e^{i\Phi}, \quad F^\mu = \int d\phi \frac{a^\mu(\phi)}{m} e^{i\Phi}, \quad S = \int d\phi \frac{a^2(\phi)}{m^2} e^{i\Phi},$$

with the exponent:

$$\Phi(\phi) = \int_{\phi_i}^{\phi} d\phi' \frac{\ell \cdot \pi_p(\phi')}{m^2 \eta_\ell (1-s)}, \quad (2)$$

where $\pi_p(\phi)$ is the instantaneous momentum of the positron in the field.

Slowly-varying Envelope Approximation: We now choose, as an example, the vector potential a^μ with circular polarisation:

$$a^\mu(\phi) = m\xi [0, \cos \Psi(\phi), \sin \Psi(\phi), 0] f(\phi), \quad (3)$$

in which $\Psi'(\phi) = \omega(\phi)/\omega_0$ is the chirped frequency of the pulse. At the initial phase, $f(\phi_i) = 0$ and $\omega(\phi_i) = \omega_0$. We request that

- i $f'(\phi) \ll 1$: the variation of the pulse local amplitude is much slower than the laser frequency
- ii $\omega'(\phi) \ll 1$: the variation of the local frequency $\omega(\phi)$ is on the same time scale as the pulse local amplitude

The exponent (2) can be expressed approximately as

$$\Phi(\phi) \approx \kappa(\phi)\phi - \zeta(\phi) \sin[\Psi(\phi) - \psi] \quad (4)$$

by ignoring all the terms proportional to $\omega'(\phi)$, $f'(\phi)$, and

$$\kappa = \frac{\ell \cdot p}{m^2 \eta_\ell (1-s)} + \frac{\xi^2}{2\eta_\ell (1-s)s} \int_0^\phi d\tilde{\phi} f^2(\tilde{\phi}), \quad \zeta = \frac{|q_\perp| \xi f(\phi) \omega_0}{\eta_\ell (1-s)s \omega(\phi)}.$$

With the Jacobi-Anger expansion:

$$e^{-i\zeta \sin(\Psi-\psi)} = \sum_{n=-\infty}^{+\infty} J_n(\zeta) e^{in\psi} e^{-in\Psi}, \quad (5)$$

where $J_n(\zeta)$ is the Bessel function of the first kind, the functions S can be expanded approximately as a series of harmonics:

$$S \approx -\xi^2 \sum_{n=-\infty}^{+\infty} e^{in\psi} \int d\phi f^2(\phi) J_n(\zeta) e^{i\Omega(\phi)}, \quad (6)$$

where $\Omega(\phi) = \kappa(\phi)\phi - n\Psi(\phi)$. The functions I and F can be calculated in the same way and obtained with the exactly same exponent term.

Stationary-phase Analysis: From (6), one can see that the main contribution to the functions I , F and S , and therefore to the final spectrum (1), comes from the *stationary phase point* where

$$\frac{\partial}{\partial \phi} \Omega(\phi) = \frac{q_\perp^2 + m_*^2(\phi)/m^2}{2\eta_\ell (1-s)s} - n \frac{\omega(\phi)}{\omega_0} = 0. \quad (7)$$

where $m_*(\phi) = m[1 + \xi^2 f^2(\phi)]^{1/2}$ is the effective mass of the produced positrons implying a chirp in the positron energy varying with the pulse envelope, $ds/d\phi \neq 0$ if $\omega(\phi) = \omega_0$.

Based on the stationary condition (7), this frequency chirp can be prescribed by solving the differential equation:

$$\frac{d\omega}{d\phi} = \frac{\omega_0}{2m\eta_\ell (1-s)s} \frac{d}{ds} [q_\perp^2 + 1 + \xi^2 f^2(\phi)], \quad (8)$$

with the initial conditions: $f(\phi_i) = 0$ and $\omega(\phi_i) = \omega_0$, and acquired with its explicit expression:

$$\omega(\phi) = \omega_0 \left[1 + \xi^2 f^2(\phi)/(q_\perp^2 + 1)\right]. \quad (9)$$

From (9), one can see a remarkable fact that this chirp prescription is irrelevant to the harmonic order n , which indicates this spectral broadening can be removed from all the harmonic lines at the same time. One should also note that the complete counterbalance of the broadening can only happen at a particular outgoing angle: $|q_\perp| \sim \gamma_p \theta_p$ specified by the chirp (9).

Numerical Result

We are interested in the on-axis positrons collimated in the direction of the incoming photon $q_\perp \rightarrow 0$ for higher yield, and thus apply the frequency chirp:

$$\omega(\phi) = \omega_0 [1 + \xi^2 f^2(\phi)]. \quad (10)$$

Inserting back into the stationary condition (7), one can then get the unchirped positron spectrum peaked at the angle $\theta_p = 0$ around the harmonic line

$$s_{n,\pm} = [1 \pm \sqrt{1 - 2/(n\eta_\ell)}]/2 \quad (11)$$

which can be understood as the linear BW harmonic in the collision between the incident photon ℓ^μ and a photon with momentum nk^μ . We employ the laser pulse with the UV frequency $\omega_0 = 15.5$ eV and the envelope $f(\phi) = \sin^2(\phi/2N)$ where $0 < \phi < 2N\pi$ and $N = 16$.

NBW: Fig. 1 depicts the narrowing of the positron angular spectra from the chirped laser pulse benchmarked with the results from constant-frequency pulses.

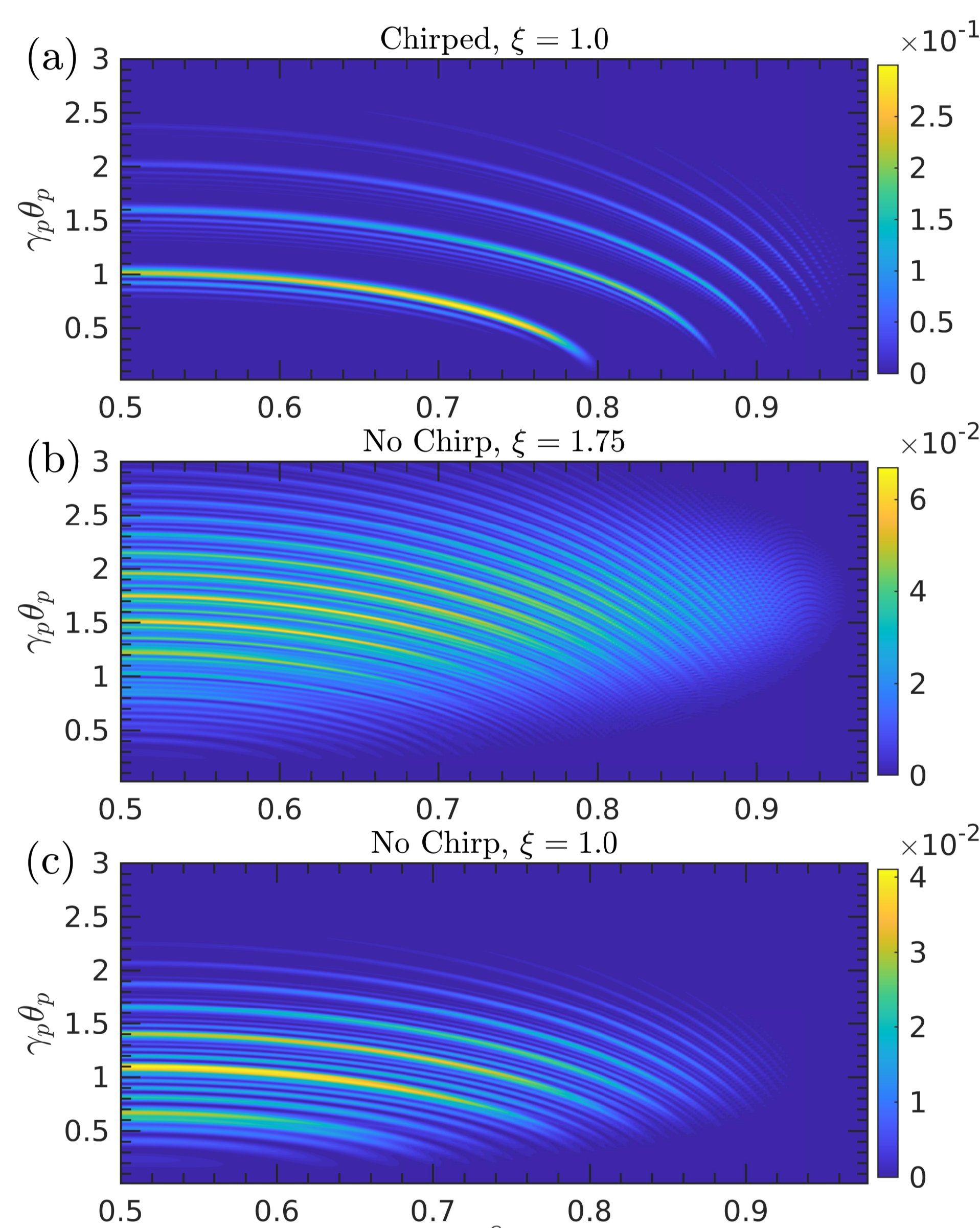


Fig. 1 Angular-energy distribution $d^2P/[ds d(\gamma_p \theta_p)]$ of the produced positrons via the NBW process from a high-energy photon (13.1 GeV) in a circularly polarised laser pulse with the proposed frequency chirp: (a) $\xi = 1$, and without the frequency chirp: (b) $\xi = 1.75$; (c) $\xi = 1$. The chirped laser pulse ($\xi = 1$, $\omega(\phi) = \omega_0[1 + \xi^2 f^2(\phi)]$) has the same energy as the unchirped laser pulse ($\xi = 1.75$, $\omega(\phi) = \omega_0$).

Fig. 2 illustrates energy spectra dP/ds of the produced positrons shown in Fig. 1 within different angular spread.

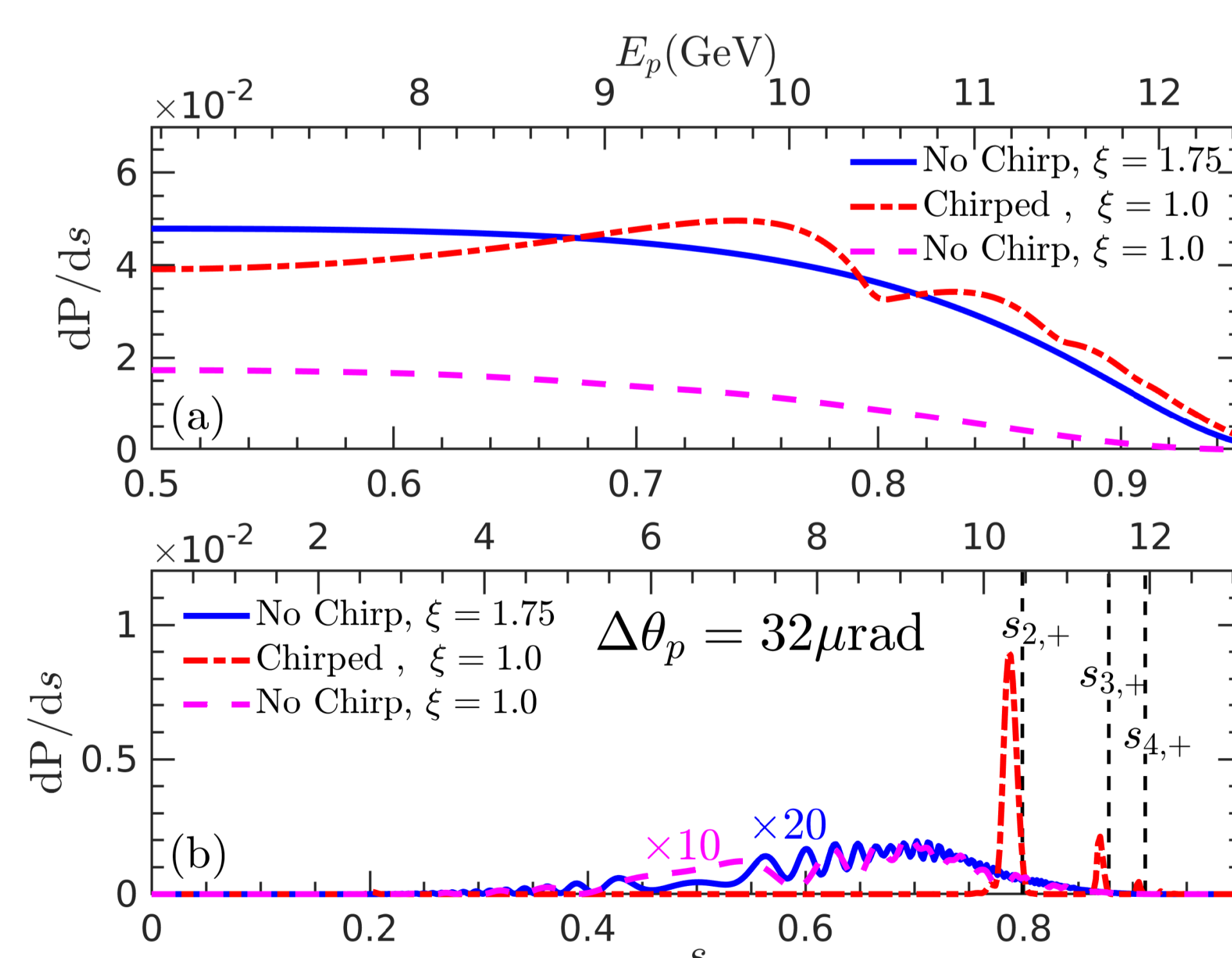


Fig. 2 Energy spectra dP/ds of the produced positrons shown in Fig. 1 within the whole angular spread: $\Delta\theta_p = \pi$ (a) and a narrow acceptance: $\Delta\theta_p = 32 \mu\text{rad}$ (b). The vertical dashed lines show the location of the first three harmonics in the chirped NBW process: $s_{2,+} = 0.80$, $s_{3,+} = 0.88$ and $s_{4,+} = 0.91$.

NLC: Fig. 3 describes the generation of quasi-monoenergetic γ -photons via the nonlinear Compton scattering process from a chirped laser pulse colliding with a beam of $E_e = 16.5$ GeV electrons [1].

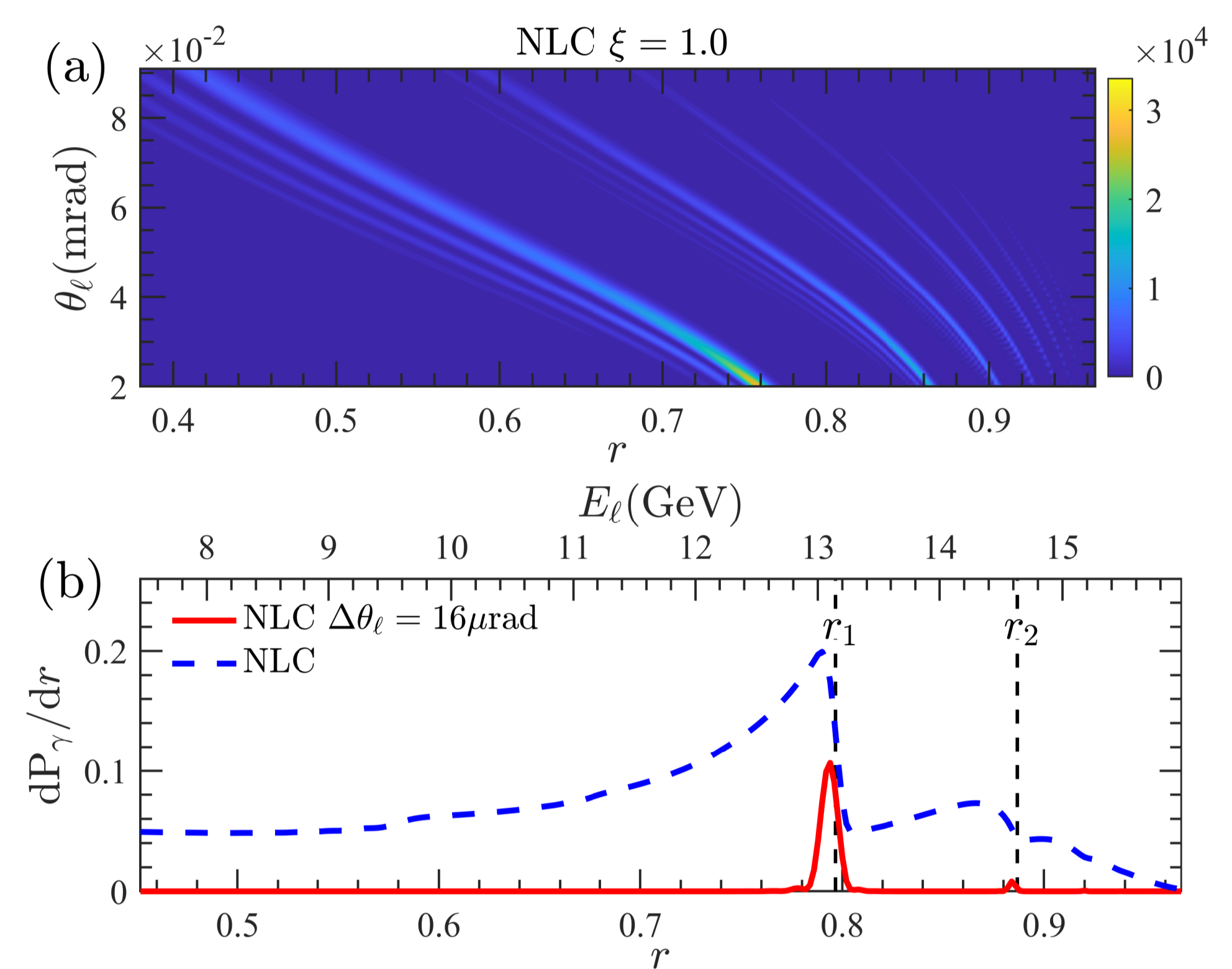


Fig. 3 (a) Angular-energy distribution $d^2P_\gamma/(dr d\theta_\ell)$ of the γ -photons generated through the NLC process from a high-energy electron $E_e = 16.5$ GeV. (b) Energy spectrum of the emitted γ -photons within the whole angular spread: $\Delta\theta_\ell = \pi$ and a narrow acceptance: $\Delta\theta_\ell = 16 \mu\text{rad}$. The vertical dashed lines show the location of the first two harmonics: $r_1 = 0.80$ and $r_2 = 0.89$, where $r = k \cdot \ell / k \cdot p_e$ is the fraction of the light-front momentum taken by the scattered photon from the seed electron.

NLC+NBW: We present a two-step scenario in which a beam of quasi-monoenergetic γ -photons is obtained from a chirped laser pulse via the NLC process and then is used to produce electron-positron pairs in the second chirped laser pulse to provide a quasi-monoenergetic source of positrons.

Making use of the obtained γ -ray spectrum: $\rho_\gamma(r) = dP_\gamma/dr$ in Fig. 3 (b), we can calculate the total number of the generated positrons:

$$P = \frac{\alpha}{(2\pi\eta_e)^2} \int_0^1 dt \int_t^1 dr \rho_\gamma(r) h(r, t) \quad (12)$$

where $t = k \cdot p / k \cdot p_e$ denotes the fraction of the light-front momentum transferring from the seed electron to the produced positron, and

$$h = \int d^2q_\perp \frac{|I|^2 + (SI^* + IS^* - 2F \cdot F^*)g(t, r)}{(r-t) r t}. \quad (13)$$

In Fig. 4, we plot the yield of the positrons from the on-axis γ -photons ($\Delta\theta_\ell = 16 \mu\text{rad}$) obtained through the NLC process, and the energy spread and location shift of the main harmonic peak:

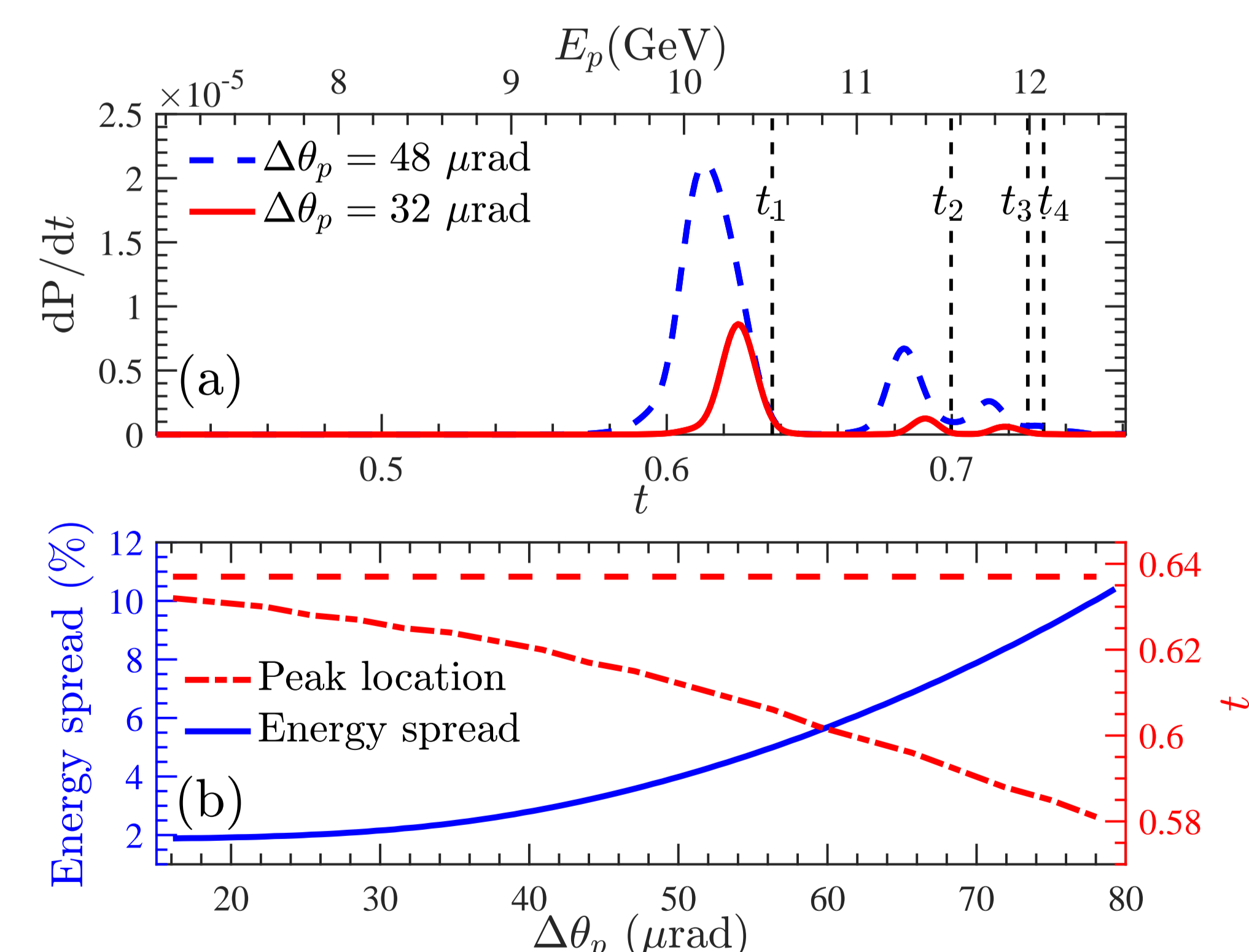


Fig. 4 Energy distribution dP/dt of the positrons generated by the on-axis γ -photons obtained through the NLC process of a high-energy electron $E_e = 16.5$ GeV. The vertical black dashed lines denote the location of each combined harmonic: $t_{1,2,3,4} = (0.637, 0.700, 0.726, 0.732)$. (b) Energy spread and peak location of the first harmonic peak with the change of the acceptance $\Delta\theta_p$. The horizontal dashed line denotes the theoretical location of the first combined harmonic: t_1 .

References

- [1] D. Seipt, S. G. Rykovanov, *et. al.*, Phys. Rev. A **91**, 033402 (2015).
- [2] Suo Tang, Phys. Rev. A **104**, 022209 (2021).